



Wang, W., Zhou, L. J., Wang, Z. W., Escaler, X., De La Torre, O., & Kang, W. Z. (2019). Dynamic response of a NACA0009 hydrofoil under cavitation conditions. In *29th IAHR Symposium on Hydraulic Machinery and Systems (IAHR2018): Proceedings of a meeting held 17-21 September 2018, Kyoto, Japan.* (Vol. 240). IOP Publishing. <https://doi.org/10.1088/1755-1315/240/6/062003>

Publisher's PDF, also known as Version of record

License (if available):
CC BY

Link to published version (if available):
[10.1088/1755-1315/240/6/062003](https://doi.org/10.1088/1755-1315/240/6/062003)

[Link to publication record in Explore Bristol Research](#)
PDF-document

This is the final published version of the article (version of record). It first appeared online via IOP at <https://doi.org/10.1088/1755-1315/240/6/062003> . Please refer to any applicable terms of use of the publisher.

University of Bristol - Explore Bristol Research

General rights

This document is made available in accordance with publisher policies. Please cite only the published version using the reference above. Full terms of use are available:
<http://www.bristol.ac.uk/pure/about/ebr-terms>

PAPER • OPEN ACCESS

Dynamic response of a NACA0009 hydrofoil under cavitation conditions

To cite this article: W Wang *et al* 2019 *IOP Conf. Ser.: Earth Environ. Sci.* **240** 062003

View the [article online](#) for updates and enhancements.



IOP | ebooks™

Bringing you innovative digital publishing with leading voices to create your essential collection of books in STEM research.

Start exploring the collection - download the first chapter of every title for free.

Dynamic response of a NACA0009 hydrofoil under cavitation conditions

W Wang¹, L J Zhou^{1,3}, Z W Wang², X Escaler⁴, O De La Torre⁵, W Z Kang¹

¹College of Water Conservancy and Civil Engineering, China Agricultural University, Beijing, 100083, China

²Department of Thermal Engineering, Tsinghua University, Beijing, 100084, China

³ Beijing Engineering Research Center of Safety and Energy Saving Technology for Water Supply Network System, Beijing, 100083, China

⁴ Department of Fluid Mechanics, Universitat Politècnica de Catalunya-Barcelona Tech, Spain

⁵ Department of Aerospace Engineering, University of Bristol, United Kingdom

E-mail: zlj@cau.edu.cn

Abstract: The dynamic response of an hydraulic machine is greatly affected by the water due to the added mass effect. However, the presence of cavitation can change the modal response of the coupled fluid-structure system because it modifies the properties of the surrounding fluid, i.e. the speed of sound and density. In this paper, a FEM-based acoustic-fluid model has been used to simulate the dynamic response of a NACA0009 hydrofoil with attached leading edge cavitation. The natural frequencies and the corresponding mode shapes have been compared for the hydrofoil in air, in still water and in cavitation conditions. The numerical predictions show a good agreement with the experimental results obtained in a high-speed cavitation tunnel. They confirm that different fluid conditions can modify the mode shapes in comparison with the modes in air. The nodal lines of the torsion and the second bending modes are slightly shifted with water and cavitation. Furthermore, the third mode of vibration under cavitation conditions appears as a combination of the torsion and the second bending shapes. The results indicate that such alterations are mainly induced by the value of the speed of sound inside the cavity.

1. Introduction

The dynamic behaviour of hydraulic machinery has to be correctly assessed during the design stage to avoid resonances. It has been demonstrated that the modal response of a structure is significantly different when submerged in water or vapor-water mixtures [1-2].

Lindholm et al. [3] analyzed the vibration of cantilever plates in air and water, showing that the fluid had a significant effect upon the dynamic plate frequencies. Kwak [4] estimated the natural frequencies of circular plates in water by using an approximate formula, which mainly depends upon the so-called added virtual mass incremental factor. Chang and Liu [5] experimentally found that the mode shapes of a plate under a flow can suffer small changes. Rodriguez et al. [6] carried out experimental modal analysis of a Francis runner submerged in still water. All these studies showed that the natural frequencies and mode shapes are not changed in a low-density fluid such as air in relation to the results in vacuum. But if the structure is submerged in a high-density fluid, the natural



frequencies are drastically reduced meanwhile the mode shapes do not differ significantly.

However, cavitation is a rather common phenomenon in hydraulic machinery that modifies the average properties of the surrounding fluid. For example, the structure might not be fully wetted and the two-phase fluid might not be homogeneous. Fine et al. [7] found that the added mass of the circular disk under a supercavitation flow is lower than under the fully wetted conditions with water. De La Torre et al. [8] investigated experimentally a 2-D NACA0009 truncated hydrofoil under cavitation conditions and concluded that the added mass decreased with cavity length. These studies mainly focused on the natural frequencies of the structures under cavitation conditions.

In reference to the hydrofoil mode shapes, De La Torre et al. [9] found experimentally slight alterations between different fluid conditions. In particular, they observed that the mode shape of the second bending mode under cavitation conditions was actually closer to a bending-torsion coupled mode, but the reason for that could not be found out. In order to understand such results, a FEM-based acoustic-fluid model has been used to simulate the dynamic characteristics of a NACA0009 hydrofoil under air conditions, still water conditions and cavitation conditions. And the obtained results and conclusions are presented in the current paper.

2. Numerical simulation

2.1. Coupled acoustic-structure modelling

FEM-based acoustic-fluid approach to simulate the added mass effect of surrounding water on a solid structure has been widely used in hydraulic turbine runners with sufficient accuracy as for example by Liang et al. [10]. In this case, the fluid-structure coupled system can be written as:

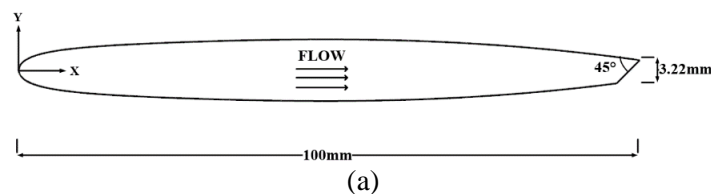
$$[M_s]\{\ddot{u}\} + [C_s]\{\dot{u}\} + [K_s]\{u\} = \{F_s\} + \{F_{fs}\} \quad (1)$$

$$[M_f]\{\ddot{p}\} + [C_f]\{\dot{p}\} + [K_f]\{p\} = \{F_f\} + \{F_{sf}\} \quad (2)$$

where, $[M_s]$ is the structural mass matrix, $[C_s]$ is the structural damping matrix, $[K_s]$ is the structural stiffness matrix, $\{F_s\}$ is the load vector on the structure, $\{u\}$ is the nodal displacement vector, $[M_f]$ is the acoustic fluid mass matrix, $[C_f]$ is the acoustic fluid damping matrix, $[K_f]$ is the acoustic fluid stiffness matrix, $\{F_{sf}\}$ is the force that the structure motion produces on the fluid, $\{F_{fs}\}$ is the force that the fluid exerts on the structure, $\{F_f\}$ is the acoustic fluid load vector and $\{p\}$ is the nodal pressure vector.

The dimensions of the NACA0009 hydrofoil were taken from the work of De La Torre et al. [8] with a truncated chord of 100mm, a span of 150mm and a trailing edge thickness of 3.22mm. The structure material was taken as aluminum with a theoretical density of 2700kg/m³, a Young's modulus of 52GPa and a Poisson's ratio of 0.3. The incidence angle of the hydrofoil was 0° as shown in Figure 1a.

De La Torre et al. [9] determined the hydrofoil mode shapes under different flow conditions from the vibration amplitudes measured at 26 points uniformly distributed on the hydrofoil surface as indicated in Figure 1b, which were excited by two PZT patches.



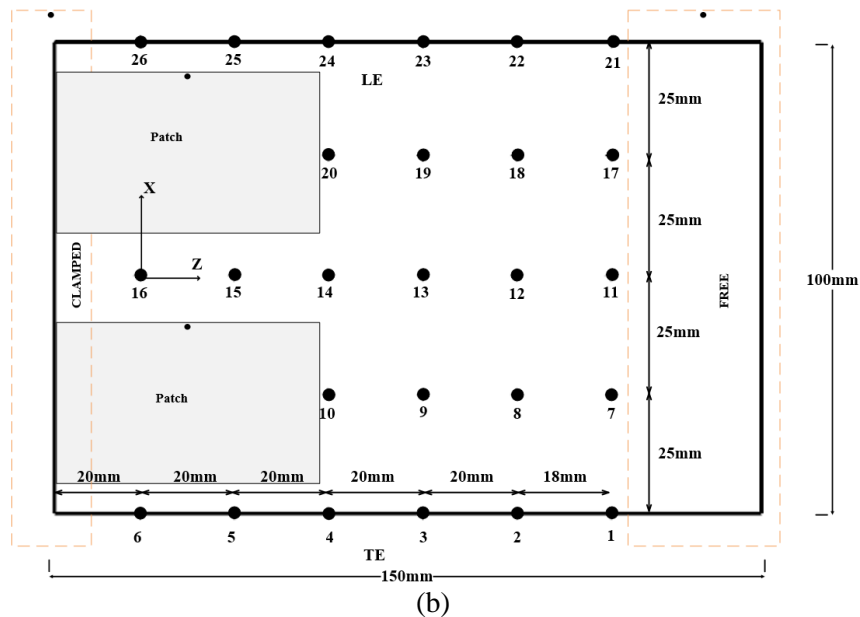


Figure 1. (a) Cross section of the hydrofoil from leading edge (left) to trailing edge (right), (b) top view of the hydrofoil and measurement points on the surface [9].

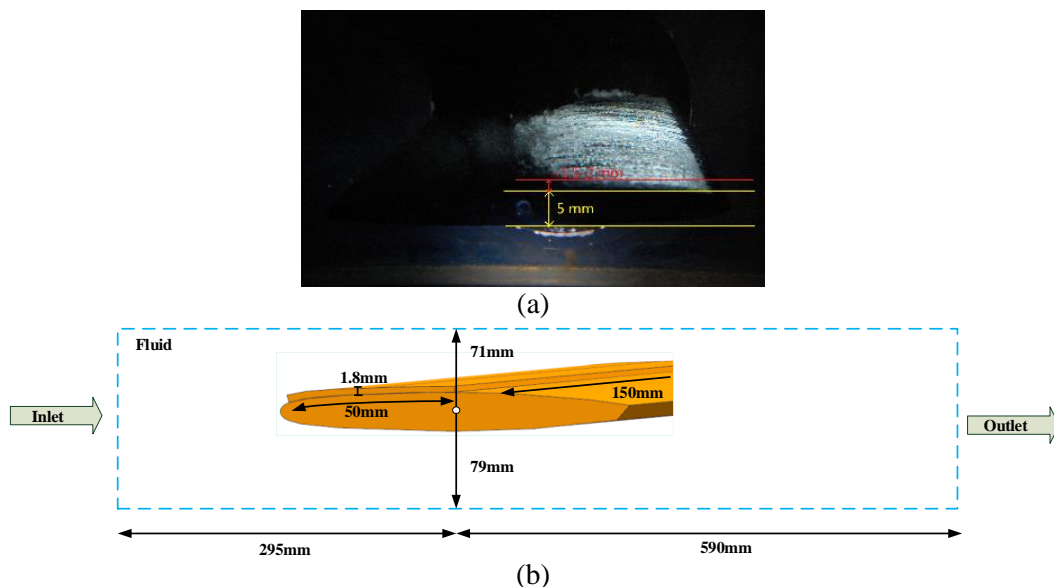


Figure 2. (a) Photograph of the attached leading edge cavitation during the tests [8], (b) outline of the model domain with main dimensions and boundary conditions.

To simulate the cavitation conditions observed during the tests (see Figure 2a), the attached vapor cavity was considered to have a constant length of 50 mm, a thickness of 1.8 mm and a span of 150 mm. The shape and location of the vapor cavity domain is shown in Figure 2b. It is assumed that the vapor cavity is stable and the dynamic change of cavitation is not considered. The acoustic properties of the elements in the cavitation domain were taken as a density of 1.205 kg/m^3 and a speed of sound of 343.21 m/s . In turn, the acoustic properties of the water domain were taken as 1000 kg/m^3 and 1450 m/s . The surrounding fluid domain corresponded to the tunnel test section dimensions of $150 \times 150 \times 885 \text{ mm}$. The flow inlet and outlet boundary surfaces were set with an absorption coefficient of 0.3. The rest of boundary surfaces were set as fully reflective. One lateral side of the hydrofoil body was fully

constrained and the opposite surface was left free to simulate a cantilever mounting. The small gap of 0.012mm between the hydrofoil tip and the lateral test section wall as modeled with acoustic elements.

2.2. Model validation

The three first natural frequencies found with the numerical model are compared in Table 1 against the experimental ones under different conditions. They correspond to the first bending mode (f_1), the torsion mode (f_2) and the second bending mode (f_3) as shown in Table 2. It is confirmed that the frequencies under still water conditions are reduced drastically compared with air conditions. However, the frequencies under cavitation conditions are slightly higher than those in still water, but they are still much lower than in air. The goodness of the model is proved since the maximum deviations are below 9%.

Table 1. Numerical and experimental natural frequencies under different conditions.

Modes	First bending f_1			Torsion f_2			Second bending f_3		
	air	water	cavitation	air	water	cavitation	air	water	cavitation
Exp. [Hz]	270	125	134	1021	625	670	1657	875	961
Sim. [Hz]	279	133	142	999	611	647	1689	949	1017
Dev. [%]	3.5	6.6	5.9	2.1	-2.2	-3.5	1.9	8.4	5.8

Table 2. Numerical mode shapes under different conditions.

Modes	Air	Still water	Cavitation
First bending f_1			
Torsion f_2			
Second bending f_3			

The relative hydrofoil deformations at f_1 , f_2 and f_3 obtained numerically are compared with the corresponding relative hydrofoil vibrations measured experimentally for air, still water and cavitation conditions in figures 3 to 5, respectively. The plots show that the simulated mode shapes are close to the measured ones. Only, slight deviations can be observed at some points, but the overall trends are in good agreement, thus confirming the accuracy of the model.

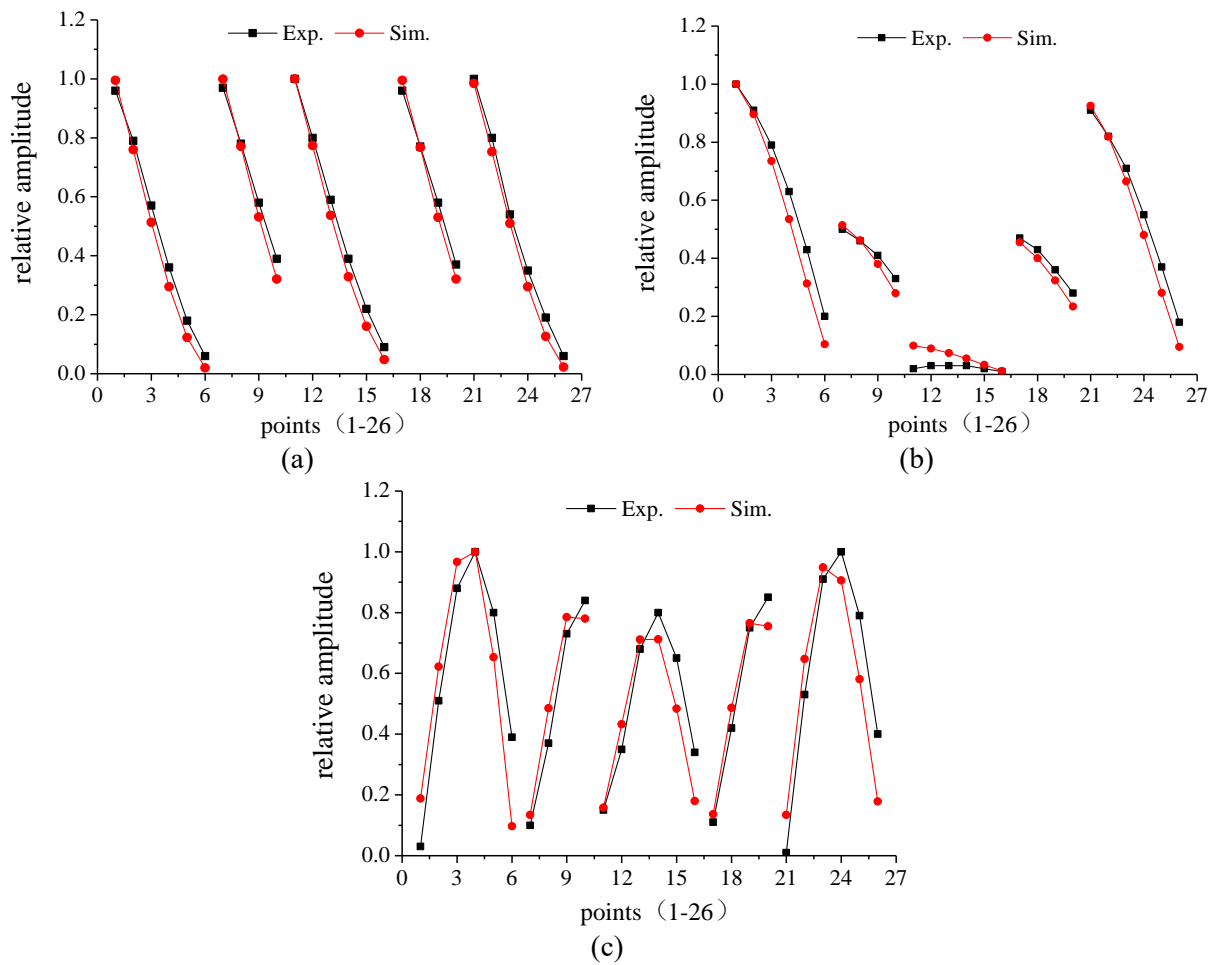
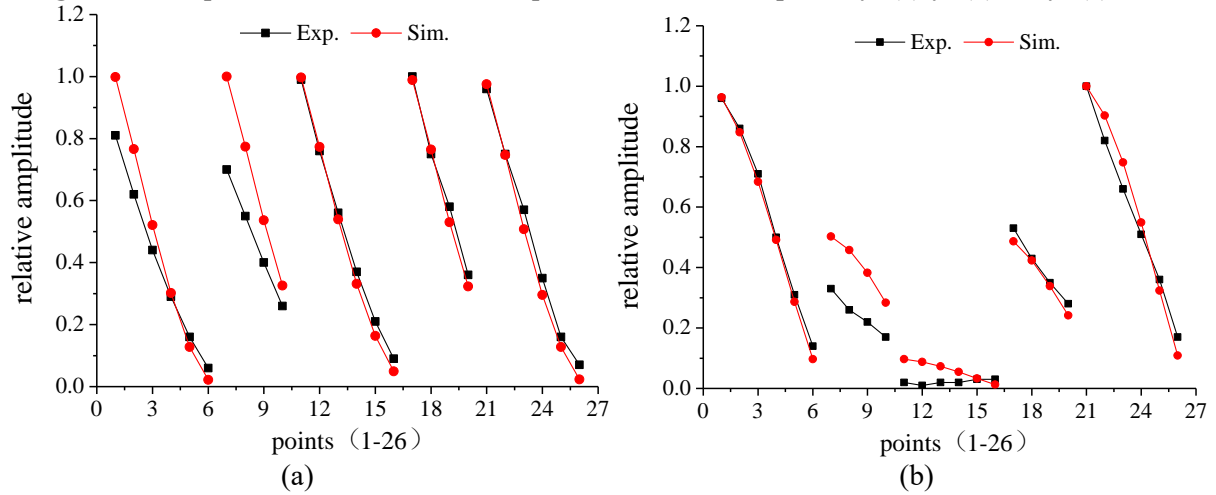


Figure 3. Comparison of numerical and experimental mode shapes for f_1 (a), f_2 (b) and f_3 (c) in air.



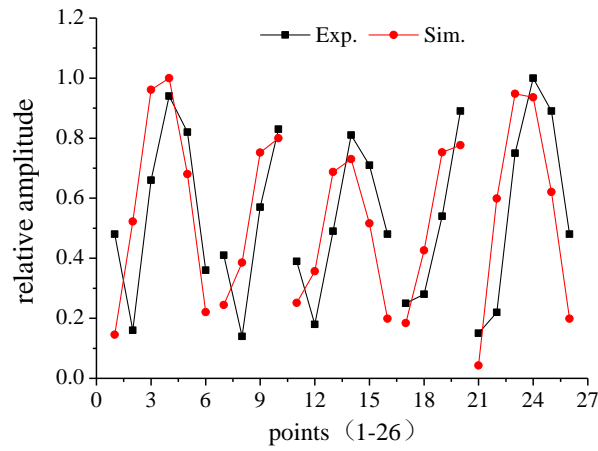


Figure 4. Comparison of numerical and experimental mode shapes for f_1 (a), f_2 (b) and f_3 (c) in still water.

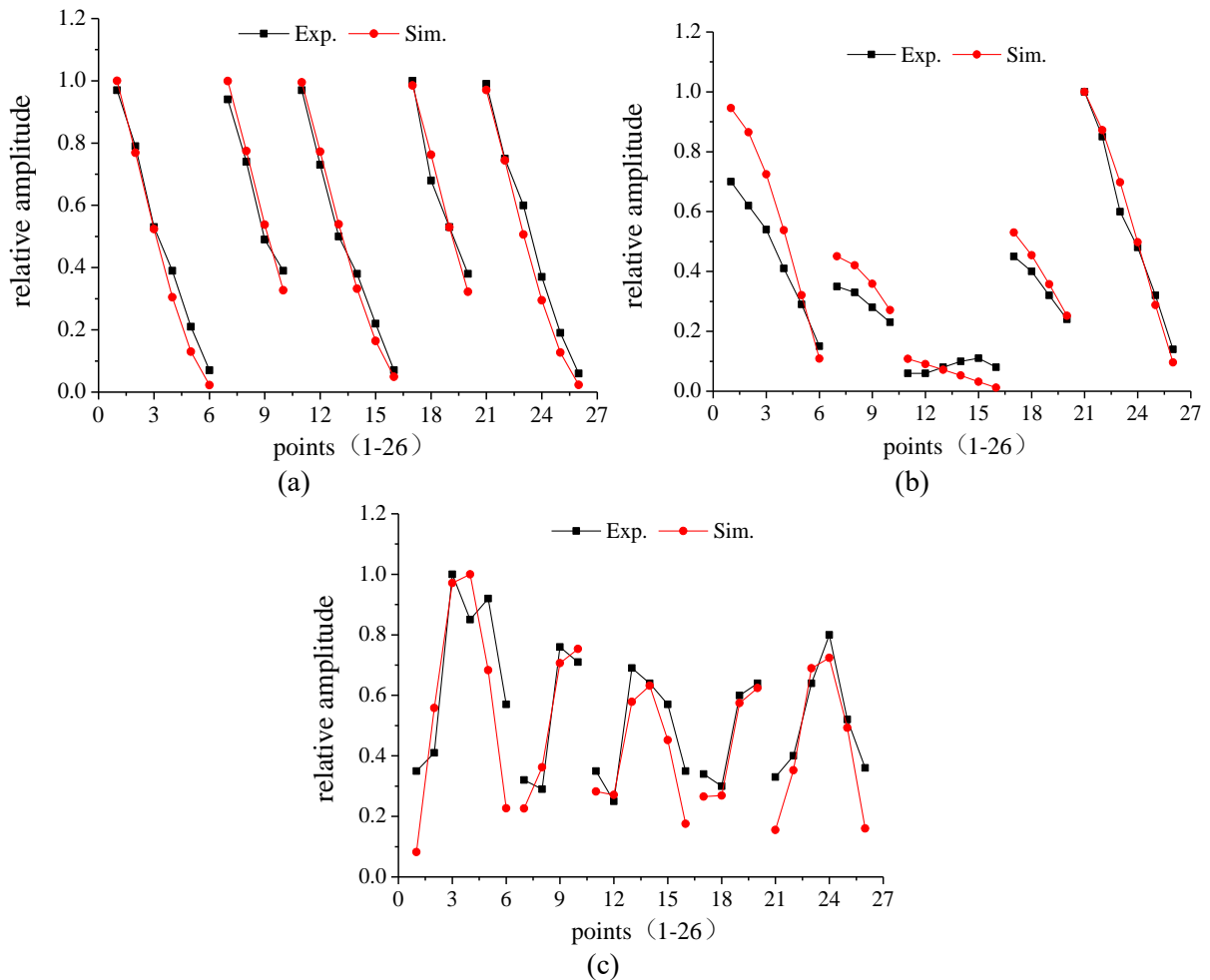


Figure 5. Comparison of numerical and experimental mode shapes for f_1 (a), f_2 (b) and f_3 (c) in cavitation.

3. Discussion

The simulated mode shapes for f_1 plotted in Table 2 do not show significant changes for the different fluid conditions. However, slight alterations of the shapes are observed for f_2 and f_3 in water and in

cavitation relative to the air results. In order to quantify such changes, a line of points in span wise direction close to the trailing edge (TE) have been selected which follows the line defined by points numbered from 1 to 6 in the experiments. In Figure 6a, the normalized deformations at TE for the torsion mode f_2 have been plotted for air, water and cavitation conditions. And in Figure 6b, the deformation at the same points have been plotted for the second bending mode f_3 also in different conditions.

The most remarkable observation is that for f_3 the zero displacement location moves along the hydrofoil span as it was already detected in the experiments. The nodal point in air is located about 76.7% of the span, with a deviation of about -0.9% from the experimental position. Then, for still water, the nodal point moves backwards towards the clamped section and it is located about 69.3%, with a deviation of -0.6% from the experimental value. For cavitation condition, the position is very close to the air condition, which is in disagreement with the experimental results that locate such point around 72.6% of the span.

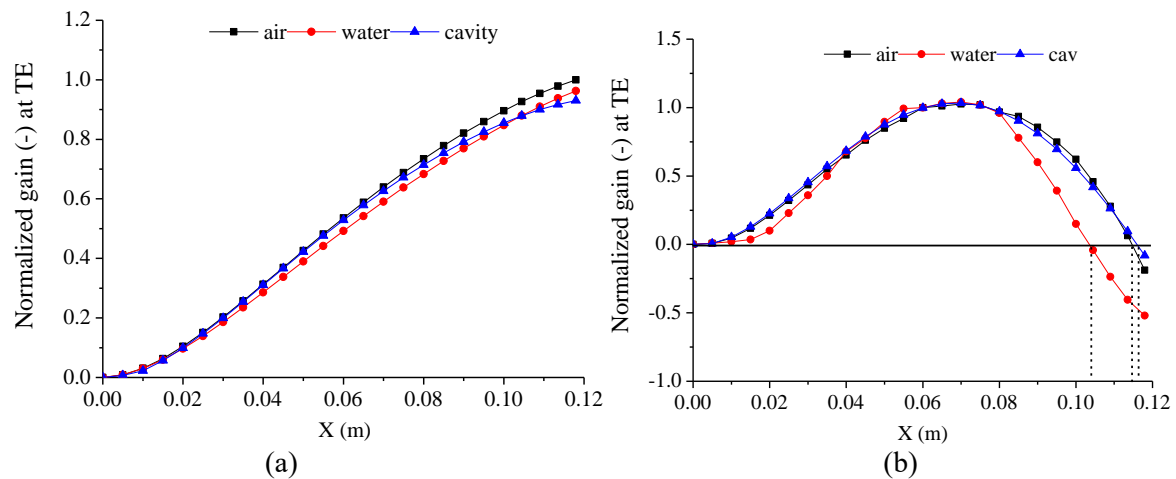


Figure 6. Normalized deformations at trailing edge for f_2 (a) and f_3 (b).

To investigate the disagreement between the nodal point location predicted by simulation for f_3 in cavitation conditions and the experimental results, the recent work of Liu et al. [11] has been considered. Their numerical results showed that the value of the speed of sound inside the cavity had a significant influence on the hydrofoil modes of vibration meanwhile the effect of changing the density was negligible. A change of acoustic properties is expected inside the cavity because the visual observations [8] pointed out that the actual cavity was a mixture of vapor and water instead of a pure vapor sheet. In this sense, Brennen [12] points out that the sound speed in a mixture of water and vapor varies with the void fraction α as plotted in Figure 7.

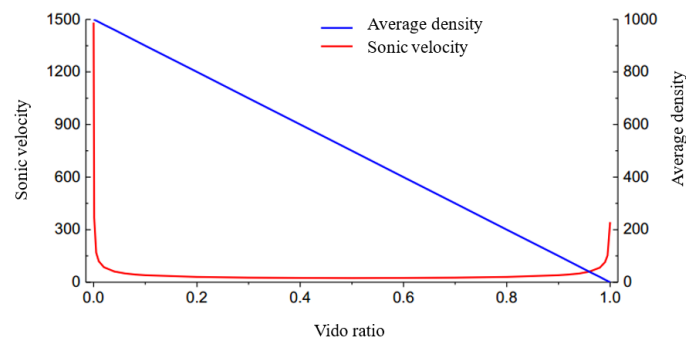
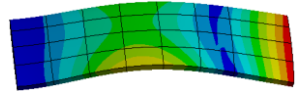
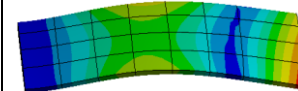
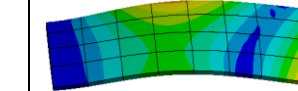


Figure 7. Speed of sound (red line) and density (blue line) as a function of void ratio α in a bubbly air/water mixture at atmospheric pressure.

Based on that, it was decided to compute the effect of α in the mode shape of mode f_3 . In particular, three values corresponding to $\alpha = 1$ ($\rho = 1.205\text{kg/m}^3$, $c = 343.21\text{m/s}$), $\alpha = 0.999$ ($\rho = 2.2\text{kg/m}^3$, $c = 270\text{m/s}$) and $\alpha = 0.9987$ ($\rho = 2.5\text{kg/m}^3$, $c = 260\text{m/s}$) were simulated. The resulting mode shapes are compared in Table 3.

Table 3. Mode shapes of f_3 for different cavity void ratios α .

$\alpha = 1.0$	$\alpha = 0.999$	$\alpha = 0.9987$
		

It can be clearly observed that a very small reduction of void ratio has a significant effect on the mode shape. As the speed of sound is decreased, the torsional deformation appears and it is increased as it can be seen at the tip of the hydrofoil. For $\alpha = 1$, all the points at the tip present maximum vertical displacement, but for lower α the displacement is maximum close to one edge and it is minimum at the opposite edge. So, the bending-torsion mode shape observed in the experiments is simulated. Moreover, the nodal line moves backwards towards the hydrofoil clamped section as shown in Figure 8. The minimum deviation of the nodal location relative to the experimental results is found when α is 0.9987 with a value of 0.9%. Additionally, the natural frequency of f_3 decreases with decreasing α meanwhile the frequency of f_1 and f_2 remains unchanged, as indicated in Table 4. And when α is 0.9987, the frequency deviation is reduced to -3.8% for f_3 . So, a very good agreement with De La Torre et al. [9] results is found for all the modal properties.

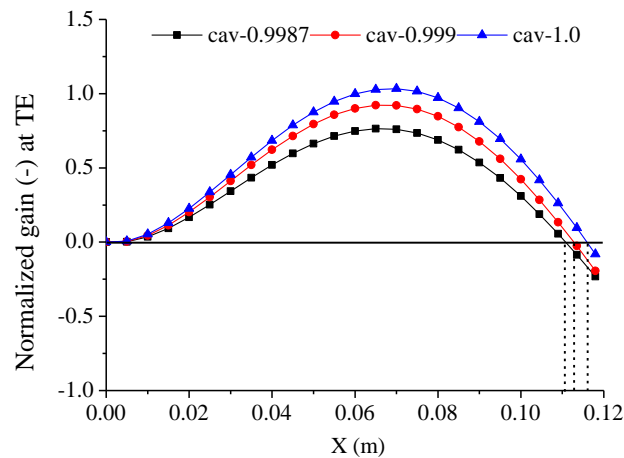


Figure 8. Normalized deformations at trailing edge for f_3 with different cavity void ratios.

Table 4. Numerical and experimental natural frequencies under cavitation conditions.

Modes	First bending f_1		Torsion f_2		Second bending f_3		
	α	1.0	0.9987	1.0	0.9987	1.0	0.9987
Exp. [Hz]		134	134	670	670	961	961
Sim. [Hz]		142	142	647	647	1017	924.1
Dev. [%]		5.9	5.9	-3.5	-3.5	5.8	-3.8

4. Conclusions

A coupled acoustic-structural FEM model was used to simulate the dynamic behavior of an hydrofoil under different flow conditions including air, still water and cavitation. The modal response obtained numerically showed a good agreement with the experimental results in terms of natural frequencies and mode shapes.

Compared with air conditions, the frequencies of the submerged hydrofoil were reduced significantly due to the added mass effect. In a cavitation flow, the frequencies were slightly higher than in still water. The mode shapes under water and cavitation conditions were slightly different than in air for the torsion and the second bending modes. They presented changes in the locations of the nodal points.

With a reduction of the cavity void fraction from 1.0 to 0.9987, so that the sound speed varied from 343m/s to 260m/s, the nodal line of the second bending mode was gradually shifted backwards to the clamped section and the natural frequency was reduced. Moreover, the observed bending-torsion mode shape found in the experiments was also simulated. In particular, the best agreement with experiment was found for $\alpha = 0.9987$.

In conclusion, the acoustic properties of the cavity appear to be relevant for the accurate determination of the hydrofoil dynamic response.

Acknowledgements

The research presented in this work was supported by National Natural Science Foundation of China (NO:51479200).

References

- [1] Blevins R D and Plunkett R 1979 *Formulas for Natural Frequency and Mode Shape* (Reinhold)
- [2] Brennen C E 1982 *Department of the Navy* 82
- [3] Lindholm U, Kana D, Chu W, Abramson H and Norman H 1965 *J. Ship Res.* **9** 11
- [4] Kwak M K 1991 *J. App. Mech.* **58** 480
- [5] Chang T and Liu M 2000 *J. Sound Vib.* **236** 547
- [6] Rodriguez C, Egusquiza E, Escaler X, Liang Q and Avellan F 2006 *J. Fluids Struct.* **22** 699
- [7] Fine N E, Uhlman J S and Kring D C 2001 *Proc. Int. Conf. on Fourth International Symposium on Cavitation (Pasadena)* p 006
- [8] De La Torre O, Escaler X, Egusquiza E and Farhat M 2013 *J. Fluids Struct.* **39** 173
- [9] De La Torre O, Escaler X, Egusquiza E and Farhat M 2015 *J. Mech. Eng. Sci.* **142** 921
- [10] Liang Q W, Rodríguez C G, Egusquiza E, Escaler X, Farhat M and Avellan F 2007 *Comput. Fluids* **36** 1106
- [11] Liu X, Zhou L, Escaler X, Wang Z, Luo Y and De La Torre O 2017 *J. Fluids Eng.* **139** 8
- [12] Brennen C E 1995 *Homogeneous Bubbly Flows* (Oxford: Oxford University Press)